Published by :
http://www.ijert.org

International Journal of Engineering Research & Technology (IJERT)
ISSN: 2278-0181
Vol. 9 Issue 12, December-2020

The Performance of a Plain Journal Textured Bearing

Moyad. B. Rajoub
Department of Mechanical Engineering
Arab Academy for Science and Technology
Alexandria, Egypt

Hassan. A. El-Gamal
Department of Mechanical Engineering
Alexandria University
Alexandria, Egypt

El-Arabi. M. Attia
Department of Mechanical Engineering
Arab Academy for Science and Technology
Alexandria, Egypt

***Abstract*— The present research work deals with studying the steady-state characteristics namely the Sommerfeld number, and the friction variable in addition to the attitude angle for plain bearing with a textured surface. A mathematical model has been put forward for the problem using the Reynolds equation governing the fluid lubrication inside the bearing. The equations have been put in their numerical forms suitable for computer solutions using Matlab by the finite difference method. It was concluded in the present work that textures improve the performance and raising load-carrying capacity. Some useful recommendations for future research work in this field of study are given in this work.**

Keywords: Hydrodynamic bearings; Textured surface; Steady performance; Load carrying capacity.

I. INTRODUCTION

Many researches have been made on the performance of plain textured journal bearings. Tala-Ighil et al [1], examined the texture location influence on the hydrodynamic journal bearing performance. A numerical modeling is used to analyze the cylindrical texture shape effect on the characteristics of a hydro- dynamic journal bearing, based on finite difference method. The bearing is operating under steady-state conditions; the applied load is constant and the parameters are calculated for a fixed eccentricity. The bearing surface is textured with cylindrical dimples. Their work has shown that the cavity (texture) increased the lubricant film thickness locally and decreased the friction force. Full texturing was ineffective in generating hydrodynamic load capacity. Partial texturing can generate hydrodynamic lift in bearing, when the texture is located in the declining part of the contact pressure field. The textured surface affects positively the cavitation zone by increasing the full film fluid region. In the complex case of a journal bearing, with both convergent (hydrodynamic pressure) and divergent (cavitation) zones, partial texturing has a minimal positive effect and full texturing has a negative effect. The textured area optimum design depends strongly on the geometrical parameters and the operating conditions of the journal bearing. Hamdvi et al [2], examined the effect of partially textured surface of hydrodynamic long journal bearing on the pressure distribution and load carrying capacity. The schematic of partially textured journal bearing represents one groove with no slip surface. By increasing the length of partially textured region from 30° to 60°, the magnitude of load capacity will increase. The results revealed, the positive effect and a significant improvement achieved for oil film pressure at eccentricity ratio (ε= 0.1 and 0.2) considering two textured angle length ($\theta_g = 30^\circ$ and $\theta_g = 60^\circ$). The effect of surface texturing on the convergent journal bearing using CFD model by finite volume method based on Navier-Stokes was examined by Tauviqirriahman et.al [3]. In particular, the investigation is focused on the generation of the pressure distribution and the load capacity. The shallow groove provides improved lubrication performance of the journal bearing. For the eccentricity ratio of 0.2, the surface texturing improves the hydrodynamic performance lubrication by increasing the load capacity. In addition to, the eccentricity ratio of 0.8, the surface texturing didn't improve the lubrication performance, even under special conditions, but it decreases the lubrication performance of journal bearing. The dynamic characteristics and stability of cylindrical textured hydrodynamic journal bearing was studied by Ganji and Kakoty [4] where the Reynolds equation was used and solved numerically by finite difference grid in an iterative scheme. Stiffness and damping coefficients of fluid film and stability parameter are found using the first-order perturbation method for different eccentricity ratios and various texture parameters like texture depth and texture density. Results indicate that the increase in texture depth improves the stability of hydrodynamic journal bearing. Texturing does not make lightly loaded bearing highly stable. The effect of texture density on stability is very prominent and the maximum stability is obtained at 20% texture density for the operating conditions. Kango et al [5] carried out a numerical comparison for the influence of spherical texture and micro-grooving (longitudinal and transverse) on friction coefficient and an average temperature of journal bearing at low and high eccentricity ratios. In their work, a comparative study on the thermal investigations for textured and grooved journal bearings has been presented; moreover, the friction force has also been calculated and compared with the friction force calculated while ignoring the cavitation zone. Using Elrod's algorithm, and the pressure is computed iteratively through Gauss–Seidel method while using modified switch function algorithm. The proposed investigation has been carried out for incompressible and steady-state laminar flow of lubricating oil. Moreover, body and inertia forces have been ignored herein. It has been observed that the texturing/grooving in the

International Journal of Engineering Research & Technology (IJERT)
ISSN: 2278-0181
Vol. 9 Issue 12, December-2020

converging portion and maximum pressure region of the bearing improves the coefficient of friction and average temperature at low and high eccentricity ratios when compared with smooth case. It has also been observed that the grooving shows maximum reduction in bearing performance parameters when compared with spherical texture. Manser et al [6] examined the combined influence of bearing surface texturing and journal misalignment on the performances of hydrodynamic journal bearings for a Newtonian lubricant in a laminar flow with constant viscosity, under the isothermal condition, taking into account assumptions that bushing is stationary and the axial movement of the shaft is neglected. A numerical analysis is performed to test three texture shapes: square, cylindrical and triangular and shaft misalignment variation in angle and degree. The Reynolds equation of a thin viscous film is solved using a finite difference scheme and a mass conservation algorithm (Jakobsson-Floberg-Olsson (JFO) boundary conditions), taking into account the presence of textures on both full film and cavitation regions. Results indicated that the fully textured bearing with flat/constant bottom dimples poorly affected the main bearing performances as compared to the smooth case, which is directed by the micro-pressure drop effect. Moreover, as the texture contour geometry increases, the micro-pressure drop effect increases, while partial texturing significantly enhances all bearing performances by the effect of the micro-pressure recovery mechanism. Particularly these facts are more noticeable at high eccentricity ratios, high misalignment degrees and when (α) approaches 0°or 180°.As the degree of misalignment increases, the maximum pressure, the leakage flow rate, the bearing load, the friction force, and the moment increase due to a decrease in the minimum film thickness, while the load attitude angle and friction coefficient decrease due to the large bearing load. A numerical and experimental analysis was carried out by Shinde et.al [7] for investigating the performance characteristics of conical shape hydrodynamic journal bearing through partial texturing (ellipsoidal shape dimples). The numerical analysis is carried out using the thin film flow physics of COMSOL Multi-physics 5.0. The ellipsoidal dimples are developed using photochemical machining. The influence of $0-90^{\circ}$textured (ellipsoidal dimple) and $90^{\circ}-180^{\circ}$ textured (ellipsoidal dimple) partial texturing on the bearing performance parameters. The dimple shape textures were prepared by using photochemical machining. The performance characteristics like fluid film pressure (FFP), load-carrying capacity (LCC), and coefficient of friction have been studied under various geometrical parameters of the ellipsoidal dimple, semi-major axis, semi-minor axis, and dimple height. The test rig consists of a rigid steel frame with a lubricant reservoir, direct current solid-state speed control unit, journal bearing assembly, and digital pressure sensor. Bearing surface with partial texturing along $90^{\circ}-180^{\circ}$ textured region results in 42.08 % enhancement in maximum FFP whereas 42.24 % enhancement in LCC as compared with smooth surface of conical shape hydrodynamic journal bearing with a maximum 52.20% reduction of coefficient of friction. Shinde and Pawar [8] examined multi-objective optimization of surface textured journal bearing. The numerical attempts are made using Taguchi's orthogonal array L27. The significance of input variable parameters on the performance characteristics is analyzed using statistical treatment analysis of variance ANOVA. Initially, static performance analysis is carried out for a plain bearing system using thin film analysis by COMSOL Multi-physics and the results are validated with the literature. In the later part, analysis of load-carrying capacity (LCC) and frictional torque (FT) is carried out for different parameters of surface texturing. The bearing performance is studied for various groove parameters versus groove location, groove height, groove width, number of grooves, and spacing between grooves. Grey relational analysis is used to find an optimal set of parameters that gives maximum load-carrying capacity and minimum frictional torque. The numerical investigations revealed that the surface texturing configuration having a groove location of 90 to 175°, groove height of 15 µm, groove width of 2.5 mm, number of grooves of 11 and 200 µm spacing between grooves gives maximum LCC value which is 51.01% greater than the baseline journal bearing. It is noted also that the most significant factors for improving LCC are groove height and groove location which contribute 51.89% and 43.54% respectively whereas the least contributing factors are a number of grooves, the spacing between grooves and width of the groove. For achieving maximum LCC and minimum FT, a multi-objective optimization - GRA method is used. The optimization solution provides the LCC of 16.9057kN which is 51.01% higher whereas FT value of 1018.88 N mm which is 9.84% lower than the baseline value. Taura [9] carried out a theoretical investigation to examine the effect of the Texture region on the static and dynamic characteristic of partially textured journal bearings, of which the texturing area is limited on the bearing surface in the circumferential direction. The load-carrying capacity and stiffness and damping coefficients of some partially textured journal bearings with the different textured regions were calculated by using a numerical model considering the effects of both fluid inertia and energy loss at the edges of the dimples. The results showed that an appropriate partial texturing formed on the bearing surface can improve both the load-carrying capacity and the stability characteristics simultaneously. The start angle of the texture region should be set at 270 from the top of the bearing in the rotating direction to improve the bearing characteristics. Lampaert et al [10], examined the potential of using the concept of rheological texture in journal bearings. The work discusses a new type of hybrid journal bearing in which a magneto-rheological fluid is used in combination with local magnetic fields so as the hydrodynamic and hydrostatic working regimes are not compromised. In addition, the work discusses a herringbone bone bearing that uses the rheological texture in a v-shaped pattern. The performance is assessed in a FEM platform (COMSOL Multiphysics® 5.4) in which the ideal Bingham plastic fluid model is used to predict the behavior of the fluid film. Their work has shown that bearing performance can be enhanced by using rheological textures. This principle adds an extra parameter in the design of a bearing that can be used to boost the performance. The results show also an increase in specific load capacity but also an increase in friction coefficient. Finally, a combined influence of textured surface and micropolar lubricant behavior was studied by Khatri and Sharma [11] worked on the performance of two-lobe hole-entry hybrid journal bearing system. In their work, the bearing performance parameters of the textured circular/two-lobe hole-entry hybrid journal bearing system have been computed against the constant vertical external load supported by the bearing. Eringen's micro-polar fluid theory has been used to derive the governing Reynolds equation. The

International Journal of Engineering Research & Technology (IJERT)
ISSN: 2278-0181
Vol. 9 Issue 12, December-2020

consequent solution of the governing Reynolds equation has been obtained by using the finite element method (FEM) numerical technique. In their analysis of the journal bearing configuration, body forces and body couples are neglected for a steady and incompressible flow of the micro-polar lubricant. Their study indicates that the use of the textured surface, two-lobe profile of bearing and micro-polar lubricant, significantly enhances the bearing performance as compared to non-textured circular journal bearing.

II. MATHEMATICAL MODEL

Fig.1 shows the journal bearing geometry and the system of coordinates used in the analysis. The current analysis assumes an incompressible Newtonian lubricant, laminar, and iso-viscous flow.

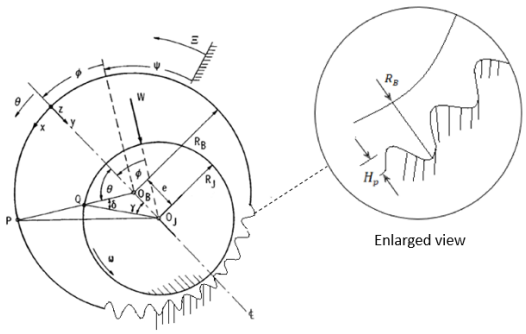

Fig.1. Journal bearing geometry with texture.

Reynolds equation governing the fluid film pressure may be written as:

$$\frac{\partial}{\partial x}\left(\frac{h^3}{\mu}\frac{\partial p}{\partial x}\right)+\frac{\partial}{\partial z}\left(\frac{h^3}{\mu}\frac{\partial p}{\partial z}\right)=6U_o\frac{\partial h}{\partial x} \qquad (1)$$

The film thickness (h) with textures may be given by the following expression:

$$h = C(1+\varepsilon\cos\theta) - \Delta(\theta, z) \qquad (2)$$

With $\varepsilon = e/C,\ 0<\varepsilon<1$

And Δ is the variation in the film thickness which written as:

$$\Delta = H_p \sin^{2m}\left\{\pi\left[\frac{\theta}{(2\pi/n_x)}-1\right]\right\}\sin^{2m}\left\{\pi\left[\frac{Z}{(L/n_z)}-1\right]\right\} \qquad (3)$$

Fig.2 shows that Δ is controlled by the protrusion height.

Where:
m: Geometry factor.
n_x: Number of protrusions in (θ) direction.
n_z: Number of protrusions in (Z) direction.
H_p: Protrusion height.

Introducing the following dimensionless variables:

$$\theta = \frac{x}{R}, \qquad \bar{z} = \frac{z}{L}$$

$$H = \frac{h}{C}, \qquad \bar{p} = \frac{p}{\mu\omega R}\left(\frac{C}{R}\right)^2 \qquad (4)$$

Here θ, $\bar{Z}$, H, and $\bar{p}$ are the dimensionless circumferential coordinate, the dimensionless axial coordinate, the dimensionless film thickness, and the dimensionless pressure, respectively.

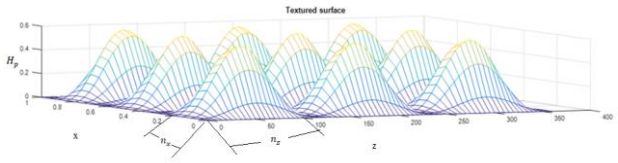

Fig.2. Texture profile.

The non-dimensional pressure equation is:

$$\frac{\partial}{\partial\theta}\left(H^3\frac{\partial\bar{p}}{\partial\theta}\right)+\left(\frac{D}{L}\right)^2\frac{\partial}{\partial\bar{z}}\left(H^3\frac{\partial\bar{p}}{\partial\bar{z}}\right)=12\pi\frac{\partial H}{\partial\theta} \qquad (5)$$

Solutions of Eq. (5) are sought subject to the Swift-Stieber boundary conditions:

$$\text{At } \bar{z}=0 \text{ and } 1, \bar{p}=0$$

$$\text{At } \theta=0 \text{ and } \theta_{eff}, \bar{p}=0 \qquad (6)$$

Swift and Stieber on the basis of a stability argument, from considerations of flow continuity at the film-cavity interface, arrived at identical conditions, namely that:

$$\text{At } \theta_{eff}, \frac{\partial\bar{p}}{\partial\theta}=0$$

$$\bar{p}=\bar{p}_{cav}=0 \text{ (For non cavitating fluid film)} \qquad (7)$$

The Swift Stieber boundary condition leads to both minimum potential energy and maximum load capacity of the bearing, and to yield minimum bearing friction. It leads to fairly good agreement with experimental data, particularly at large eccentricities, and is easy to incorporate into most numerical schemes. The components W_R and W_T in radial and transverse, respectively of the pressure force are given by:

$$W_R = \int_0^L\int_0^{\theta_{eff}} p\cos\theta\, R\, d\theta\, dz \qquad (8)$$

$$W_T = \int_0^L\int_0^{\theta_{eff}} p\sin\theta\, R\, d\theta\, dz \qquad (9)$$

Here θ_{eff} represents the angular position of the trailing edge of the lubricant film.

The load carrying capacity will be,

$$W = (W_R^2 + W_T^2)^{1/2} \qquad (10)$$

International Journal of Engineering Research & Technology (IJERT)
ISSN: 2278-0181
Vol. 9 Issue 12, December-2020

And the attitude angle is given by:

$$\emptyset = \arctan\left(\frac{W_T}{W_R}\right) \quad (11)$$

The bearing Sommerfeld number is defined as:

$$S = \frac{\mu N}{W/_{2RL}}\left(\frac{R}{C}\right)^2 \quad (12)$$

The friction force is given by:

$$F = \mu \int_0^L \int_0^{\theta_{eff}} \left.\frac{\partial u}{\partial y}\right|_{y=0} R d\theta dZ \quad (13)$$

The friction variable is defined as:

$$f\frac{R}{C} = \frac{F}{W}\left(\frac{R}{C}\right) \quad (14)$$

III. NUMERICAL ANALYSIS

The numerical scheme presented is adopted to solve the steady lubrication equation in order to determine the steady-state characteristics namely the Sommerfeld number, and the friction characteristics in addition to the attitude angle for plain bearing with a textured surface. The numerical solution used the finite difference method with the aid of the Gauss-seidel [12] successive relaxation method using a mesh size (6 degrees) and (0.017) in tangential and axial directions respectively. A relative error of less than (0.01) is to be achieved. A MATLAB program is designed in order to numerically solve the problem and to calculate the bearing performance characteristics

IV. RESULTS AND DISCUSSION

Figs 3- 13 show the pressure distribution inside the plain textured journal bearing and the variation of the bearing performance parameters namely Sommerfeld number, friction variable and attitude angle at different eccentricity ratios with the dimensionless Protrusion height, and number of protrusions.

Fig.3 and Fig.4 show the dimensionless pressure distribution for the bearing along circumferential and axial directions respectively. This is for a moderate eccentricity ratio of 0.6.

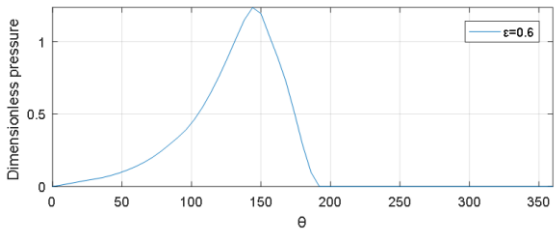

Fig.3. The dimensionless pressure distribution along circumferential direction.

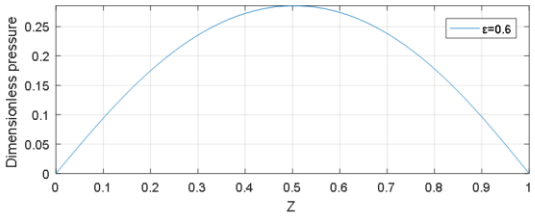

Fig.4. The dimensionless pressure distribution along the axial direction.

Fig.5 to Fig.7 shows the variation of Sommerfeld number, friction variable, and attitude angle for plain journal bearing respectively with eccentricity ratio. It is to be noted that the values of the Sommerfeld number, friction variable, and attitude angle decreased as the eccentricity ratio increased as is the case with plain non-textured journal bearing.

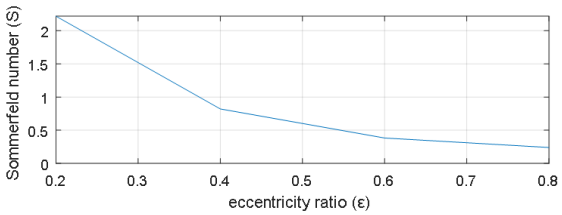

Fig.5. The variation of Sommerfeld number with eccentricity ratio for plain journal bearing.

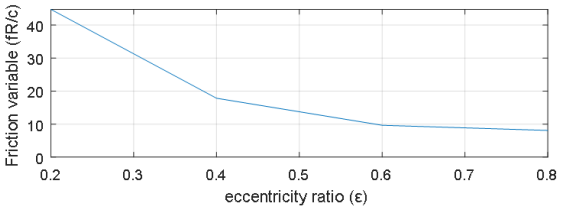

Fig.6. The variation of friction variable with eccentricity ratio for plain journal bearing.

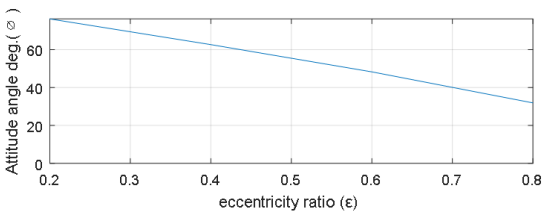

Fig.7. The variation of attitude angle with eccentricity ratio for plain journal bearing.

International Journal of Engineering Research & Technology (IJERT)
ISSN: 2278-0181
Vol. 9 Issue 12, December-2020

Fig.8 to Fig.10 shows the variation of dimensionless Protrusion height with Sommerfeld number, friction variable, and attitude angle, for the textured journal bearing respectively. This is for $\varepsilon = 0.6$. These figures show that the Sommerfeld number, friction variable, and attitude angle improved with the increasing of dimensionless Protrusion height. As is clear for zero protrusion height that is for plain journal bearing the increase in Sommerfeld number when compared to a textured one say of dimensionless protrusion height of 0.1 is about 7.32%. This means that an improvement occurs in dimensionless load carrying capacity. A similar improvement of about 5.94% in the friction variable is present.

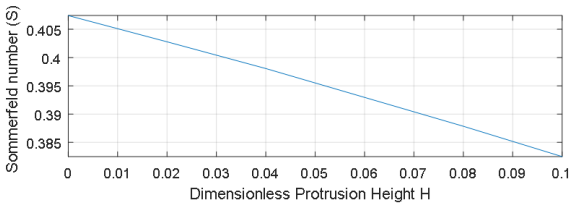

Fig.8. The variation of Sommerfeld number with dimensionless Protrusion height for $\varepsilon = 0.6$.

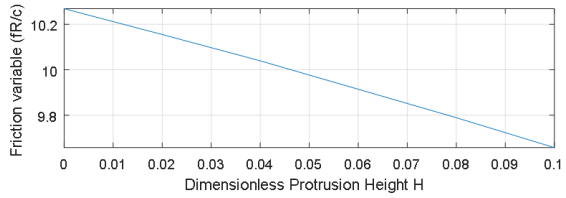

Fig.9. The variation of friction variable with dimensionless Protrusion height with $\varepsilon = 0.6$.

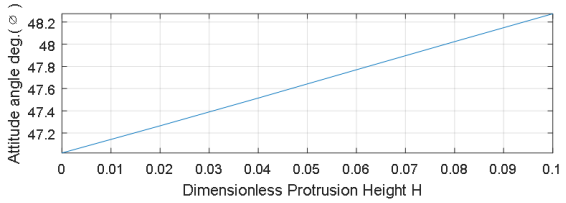

Fig.10. The variation of attitude angle with dimensionless Protrusion height with $\varepsilon = 0.6$.

Fig.11 to Fig.13 show the variation of number of protrusions in axial and circumferential directions with Sommerfeld number, friction variable and attitude angle, for textured journal bearing respectively. As it is considered from the outset that the number of protrusions in axial and circumferential directions are equal ($n_z = n_x$).

These figures show that the effect of the number of protrusions on (S) is noticeable from Fig 11. As the number increases the Sommerfeld number does not change considerably and the even number of protrusions gives somewhat lesser values of S compared to the odd ones. This is applicable to the range from 6 to 11 protrusions. From 12 to 20 protrusions the opposite holds. However it is remarkable that the number of protrusions whether it is odd or even does not have an appreciable difference on the performance as is clear from 20 to 30 protrusions. However the effect of the number of protrusions becomes more pronounced as it increases causing Sommerfeld number to increase meaning a decrease in the dimensionless load carrying capacity.

It is worth noting in this respect that the continuous increase in the number of protrusions say over 30 whether it is even or odd indicates that an asymptotic maximum value of (S) can seemingly be reached. Fig 12 shows the variation of the friction variable (f R/c) with the number of protrusions. It can be seen in general that the larger the number of protrusions the larger the friction variable. It can thus be seen that increasing the number of protrusions has an adverse effect on both load carrying capacity and friction characteristics of the bearing. Fig 13 shows the variation of the attitude angle with the number of protrusions. The order of magnitude of the variation in the attitude angle is seen to be quite negligible.

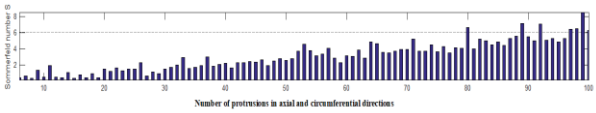

Fig.11. The variation of Sommerfeld number with number of protrusions with $\varepsilon = 0.6$.

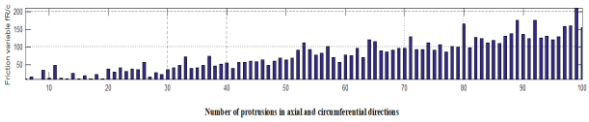

Fig.12. The variation of friction variable with number of protrusions with $\varepsilon = 0.6$.

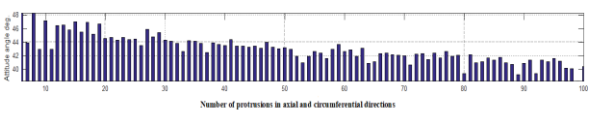

Fig.13. The variation of attitude angle with number of protrusions with $\varepsilon = 0.6$.

International Journal of Engineering Research & Technology (IJERT)
ISSN: 2278-0181
Vol. 9 Issue 12, December-2020

V. CONCLUSIONS

The following conclusions are drawn:

1- The effect of increasing the eccentricity ratio is seen to improve the dimensionless load-carrying capacity, in which the Sommerfeld number and friction variable decreased as is the case with plain non-textured journal bearing.
2- The effect of increasing the dimensionless protrusion height in textured journal bearing improved the dimensionless load-carrying capacity. Improvement of about 7.32% occurred in Sommerfeld number when compared to plain journal bearing. A similar improvement of about 5.94% in the friction variable is present.

3- Finally, the dimensionless load carrying capacity is improving from 6 to 11 protrusions for even number compared to the odd ones. From 12 to 20 protrusions the opposite holds. There is no difference in the performance from 20 to 30 protrusions whether it is an odd number or even number. It is worth noting in this respect that the continuous increase in the number of protrusions say over 30 whether it is even or odd indicates that an asymptotic maximum value of Sommerfeld number can seemingly be reached. It can be seen in general that the larger the number of protrusions the larger the friction variable. This means that the larger the number of protrusions the larger the adverse effect on both load carrying capacity and friction characteristics of the bearing.

VI. SUGGESTIONS FOR FUTURE WORK

For future work, it is suggested to carry out the following:

1- A generalization of the present work to include the thermal effects on textured journal bearing performance.

2- Extension of the present work to include the effect of elastic deformation in textured journal bearings.

3- Experimental work on textured journal bearings is very much required in general.

VII. NOMENCLATURE

Latin symbols

c	Radial clearance, m
e	Eccentricity, m
h	Film thickness, m
H	Dimensionless film thickness
n_x	Number of protrusions in (θ) direction
n_z	Number of protrusions in (Z) direction
m	Geometry factor
$\bar{Z}$	Dimensionless axial coordinate
H_p	Protrusion height, m
F	Friction force, N
W_R, W_t	Radial and transverse pressure force, N/m
W	Load carrying capacity, N
p	Pressure, Pa
$\bar{p}$	Dimensionless pressure
S	Sommerfeld number
$f\frac{R}{c}$	Friction variable
L	Bearing length, m
R_j, R_B	Journal radius and Bearing radius, m
(x, y, z)	Cartesian coordinate system

Greek Symbols

$\Delta(\theta, z)$	Variation of the film thickness, m
ε	Eccentricity ratio $\varepsilon = e/c$
θ_{eff}	Angular position of the trailing edge of the lubricant film, rad
μ	Lubricant viscosity, $P_a S$
$\emptyset$	Attitude angle, rad

VIII. REFERENCES

[1] Tala-Ighil, N., Fillon, M., and Maspeyrot, P., 2011, "Effect of Textured Area on the Performances of a Hydrodynamic Journal Bearing," Tribol. Int., Vol. 44(3), pp. 211–219.
[2] Hamdavi, S., Ya, H. H., and Rao, T. V. V. L. N., 2016, "Effect of Surface Texturing on Hydrodynamic Performance of Journal Bearings," ARPN J. Eng. Appl. Sci., Vol. 11(1), pp. 172–176.
[3] Tauviqirrahman, M., Akbar, R. A., and Hilmy, F., 2018, "The Effect of Textured Surfaces on the Hydrodynamic Pressure Generation in Journal Bearings," MATEC Web of Conferences,IMIEC, Vol. 204(6), pp. 4–9.
[4] Ganji, T. S. R., and Kakoty, S. K., 2014, "Dynamic Characteristics and Stability of Cylindrical Textured Journal Bearing,"International Journal of Recent advances in Mechanical Engineering (IJMECH). Vol. 3(3).
[5] Kango, S., Sharma, R. K., and Pandey, R. K., 2014, "Comparative Analysis of Textured and Grooved Hydrodynamic Journal Bearing," Proc. Inst. Mech. Eng. Part J J. Eng. Tribol., Vol. 228(1), pp. 82–95.
[6] Manser, B., Belaidi, I., Hamrani, A., Khelladi, S., and Bakir, F., 2019, "Performance of Hydrodynamic Journal Bearing under the Combined Influence of Textured Surface and Journal Misalignment: A Numerical Survey," Comptes Rendus - Mec., Vol. 347(2), pp. 141–165.
[7] Shinde, A., Pawar, P., Shaikh, P., Wangikar, S., Salunkhe, S., and Dhamgaye, V., 2018, "Experimental and Numerical Analysis of Conical Shape Hydrodynamic Journal Bearing with Partial Texturing," Procedia Manuf., Vol. 20, pp. 300–310.
[8] Shinde, A. B., and Pawar, P. M., 2017, "Multi-Objective Optimization of Surface Textured Journal Bearing by Taguchi Based Grey Relational Analysis," Tribol. Int., Vol. 114, pp. 349–357.
[9] Taura, H., 2019, Effect of Texture Region on the Static and Dynamic Characteristic of Partially Textured Journal Bearings, Springer International Publishing, pp.422-436
[10] Lampaert, S. G. E., Quinci, F., and van Ostayen, R. A. J., 2019, "Rheological Texture in a Journal Bearing with Magnetorheological Fluids," J. Magn. Magn. Mater., Vol. 499, p. 166218.
[11] Khatri, C. B., and Sharma, S. C., 2017, "Behaviour of Two-Lobe Hole-Entry Hybrid Journal Bearing System under the Combined Influence of Textured Surface and Micropolar Lubricant," Ind. Lubr. Tribol., Vol. 69(6), pp. 844–862.
[12] Smith G.D., Numerical solution of partial differential equations: finite difference method. Clarendon Press Oxford, 1993.